Chin. Geogra. Sci. 2017 Vol. 27 No. 4 pp. 600–613
doi: 10.1007/s11769-017-0880-z

Springer Science Press
www.springerlink.com/content/1002-0063

Spatio-temporal Variations in Plantation Forests' Disturbance and Recovery of Northern Guangdong Province Using Yearly Landsat Time Series Observations (1986–2015)

SHEN Wenjuan[1, 2], LI Mingshi[1, 2], WEI Anshi[3]

(1. *College of Forestry*, *Nanjing Forestry University*, *Nanjing* 210037, *China*; 2. *Co-Innovation Center for Sustainable Forestry in Southern China*, *Nanjing Forestry University*, *Nanjing* 210037, *China*; 3. *Guangdong Provincial Center for Forest Resources Monitoring*, *Guangzhou* 510173, *China*)

Abstract: Forest disturbance plays a vital role in modulating carbon storage, biodiversity and climate change. Yearly Landsat imagery from 1986 to 2015 of a typical plantation region in the northern Guangdong province of southern China was used as a case study. A Landsat time series stack (LTSS) was fed to the vegetation change tracker model (VCT) to map long-term changes in plantation forests' disturbance and recovery, followed by an intensive validation and a continuous 27-yr change analysis on disturbance locations, magnitudes and rates of plantations' disturbance and recovery. And the validation results of the disturbance year maps derived from five randomly identified sample plots with 25 km^2 located at the four corners and the center of the scene showed the majority of the spatial agreement measures ranged from 60% to 83%. A confusion matrix summary of the accuracy measures for all four validation sites in Fogang County showed that the disturbance year maps had an overall accuracy estimate of 71.70%. Forest disturbance rates' change trend was characterized by a decline first, followed by an increase, then giving way to a decline again. An undulated and gentle decreasing trend of disturbance rates from the highest value of 3.95% to the lowest value of 0.76% occurred between 1988 and 2001, disturbance rate of 4.51% in 1994 was a notable anomaly, while after 2001 there was a sharp ascending change, forest disturbance rate spiked in 2007 (5.84%). After that, there was a significant decreasing trend up to the lowest value of 1.96% in 2011 and a slight ascending trend from 2011 to 2015 (2.59%). Two obvious spikes in post-disturbance recovery rates occurred in 1995 (0.26%) and 2008 (0.41%). Overall, forest recovery rates were lower than forest disturbance rates. Moreover, forest disturbance and recovery detection based on VCT and the Landsat-based detections of trends in disturbance and recovery (LandTrendr) algorithms in Fogang County have been conducted, with LandTrendr finding mostly much more disturbance than VCT. Overall, disturbances and recoveries in northern Guangdong were triggered mostly by timber needs, policies and decisions of the local governments. This study highlights that a better understanding about plantations' changes would provide a critical foundation for local forest management decisions in the southern China.

Keywords: plantation; Landsat dense time series; remote sensing; forest disturbance and recovery; driving forces; northern Guangdong

Citation: Shen Wenjuan, Li Mingshi, Wei Anshi, 2017. Spatio-temporal variations in plantation forests' disturbance and recovery of northern Guangdong Province using yearly Landsat time series observations (1986–2015). *Chinese Geographical Science*, 27(4): 600–613. doi: 10.1007/s11769-017-0880-z

1 Introduction

Disturbance is an important component in forest ecosystem dynamic change. Several studies pointed out disturbance types, intensity and size impacted the growth of forest stand, tree species and forest structure (Pflug-

Received date: 2016-03-10; accepted date: 2016-07-08

Foundation item: Under the auspices of the '948' Project sponsored by the State Forestry Administration (SFA) of China (No. 2014-4-25), National Natural Science Foundation of China (No. 31670552, 31270587), Doctorate Fellowship Foundation of Nanjing Forestry University, the PAPD (Priority Academic Program Development) of Jiangsu Provincial Universities, Graduate Research and Innovation Projects in Jiangsu Province (No. KYLX15_0908)

Corresponding author: LI Mingshi. E-mail: nfulms@njfu.edu.cn

macher *et al.*, 2012; Edwards *et al.*, 2014; Cohen *et al*., 2016). For example, natural disturbance (thunderstorm, snow disaster and insects, *etc*.), human disturbance (logging/harvesting, land use change, *etc*.) were forest carbon sources and post-disturbance regeneration would cause forest carbon sink events (Turner *et al*., 2015). Also, different landscape levels, such as urbanization, climate or disaster and forest management activities, would result in different disturbance magnitudes (Kennedy *et al.*, 2015). Forest harvesting as an important characterization of human disturbance and landscape dynamics holds a robust relation with carbon storage and forest cover density, species, topography and socio-economic (Levers *et al*., 2014; Wu *et al.*, 2016).

Plantations' carbon sink in the southern China accounts for 65% of the forest carbon sink in China (Piao *et al.*, 2009). Expanding current area of the plantations can alleviate the CO_2 concentration in the atmosphere, thus mitigating the global climate warming (Fang and Chen, 2001; Ma *et al*., 2013). Since 1980, the large-scale afforestation projects have made China distribute the largest area of plantation, accumulating a quarter of global plantation area. However, the plantations include the characters of limited tree species, irrational structures and vulnerability to diseases and insects (Chen *et al*., 2014), largely constraining the carbon sequestration of the plantations ecosystem and being difficult in meeting contemporary timber demand in China. Because of the characters of fast-growing, high yield and short rotation cycle of the plantations, a widespread and frequent forest spatio-temporal change is definitely existing, which demands abrupt forest change monitoring (Huang and Zhang, 2009). For example, prompt plantations reforestation followed by a harvesting event occurs frequently in southern China. This sharp change event would be spectrally undetectable when using two or three Landsat images (Mas 1999; Coppin *et al.*, 2004; Lu *et al.*, 2004) with a long time interval. Free access of long time series Landsat images (Woodcock *et al.*, 2008) make detecting forest disturbance events over the last several decades possible. The temporal and spatial coverage, moderate spatial resolution, and long history of earth observations provide a unique opportunity for observing vegetation changes across large areas and long time scales (Masek *et al.*, 2013). Monitoring when and where forest disturbance and recovery occur by using Landsat images has a profound significance for forest management and carbon prediction, due to quantitative and spatio-temporally explicit information on forest disturbance and recovery can be derived from the monitoring process.

Forest disturbance in the current work was defined as any event that caused either substantial mortality or leaf-area reduction within a forest stand, including management activities such as harvest and thinning. Forest recovery was defined as post-disturbance recovery. Landsat time series data based algorithms (Woodcock *et al.*, 2008; Roy *et al*., 2014) captured the duration and magnitude of different disturbance types. VCT has been reported to identify the abrupt disturbance events successfully, such as forest fires, harvesting (Masek *et al*., 2013). LandTrendr is designed to detect both abrupt events as well as slower, longer-term changes across all lands (Schroeder *et al.*, 2012). Harvesting is a frequent disturbance event in plantation forests in southern China, especially for commercial forests. And the near annual records of plantation forests disturbance or recovery in southern China from 1986 to 2015 were rare. A noticeablething regarding to VCT was how to select non- contamination growing season's images to minimize phenology and BRDF differences and make multitemporal image differencing, otherwise, VCT-based mapping disturbance events displays according to the pre-establish software modules, so in situ algorithm cannot be adjusted to the user-defined function flexibly (Kennedy *et al.*, 2010). However, VCT has been proved having the advantages in both identification and mapping forest disturbance and being more robust to noise from registration, BRDF, and seasonal effects (Huang *et al.*, 2010). Additionally, the VCT model has been used to produce disturbance products for the sites where LTSS were assembled during the NAFD project (Goward *et al.*, 2008; Huang *et al.*, 2009; Huang *et al.*, 2010; Thomas *et al*., 2011), or through the LANDFIRE project (Li *et al.*, 2009a; Li *et al.*, 2009b). Noticeably, Both VCT and LandTrendr algorithms were able to find most of the major disturbances. Comparison of VCT and LandTrendr algorithms for disturbance detection have only been reported in Schroeder *et al.*, 2014. Here, there would be a trial demonstration to monitor forest disturbance or recovery based on both algorithms in Fogang County, northern Guangdong, because large commercial forests disturbance distribution could be derived from local abundant field forest survey data, however, refer-

ence data outside of Fogang were unavailable.

The aim of this study was to assess the utility of Landsat time series algorithms for mapping forest disturbance and recovery in northern Guangdong region. Our methodology comprised four main steps: 1) converting the original scenes in the stack from Beijing satellite remote sensing ground station (BJGS) in China and United States Geological Survey (USGS) to the standard surface reflectance images by the LEDAPS algorithm; then 2) characterizing forest disturbance and recovery events through analyzing forest disturbance and recovery occurrence year and rates based on VCT models; 3) monitoring and comparing forest disturbance or recovery based on VCT and LandTrendr in Fogang County; and 4) finally, evaluating the disturbance identification accuracy of VCT model and identifying the driving forces contributing to plantations' forest disturbance and recovery in the southern China.

2 Materials and Methods

2.1 Study site and data

Fig. 1 illustrates the location of the study area, with a WRS path/row number 122/043 (p122r043), covering the central and northern portions of Guangdong Province, including Shaoguan, Qingyuan and Heyuan cities. The study area extends from 113.10°E to 114.75°E and 23.64°N to 25.44°N. The local topography is undulating and its elevation is between 22 m and 1353 m above sea level. The climate is a mid-subtropical monsoon climate, with an average annual precipitation ranging from 1300 mm to 2400 mm and an average annual temperature ranging from 18℃ to 21℃. The rainy season takes place from March to August, with approximately 53% of the annual rain falling between April and June. Forest types are dominated by evergreen forests mainly composed of *Pinus massoniana*, *Cunninghamia Lanceolata*, *Pinus Elliottii Engelm*, *Cryptomeria fortunei*, *Eucalyptus*, *Pinus kwangtungensis*, *Castanopsis fissa*, *Acacia mangium*, *Populus tremula*, along with other minor tree species, as well as *Phyllostachys pubescens*, and a small amount of deciduous trees and shrubs. Fogang County in Qingyuan City is located in the southern place of the whole region, where commercial plantations were distributed (Fig. 1). Guangdong Provincial Center for Forest Resources Monitoring provided forest resources survey database ranging from 2005 to 2011 and sub-compartment data in 2005, 2006, 2009, 2011 in Fogang County to aid the identification of local forest types and non-forest types.

Thirty-one georectified Landsat 5 Thematic Mapper (TM), Landsat 7 Enhanced Thematic Mapper plus (ETM+) and Lansat 8 Operational Land Imager (OLI) images (30 m spatial resolution) from the USGS Landsat archive and BJGS for the p122r043 that spanning from 1986 to 2015 were used to characterize forest disturbance and recovery histories (Table 1). The forest management data on logging, regeneration, and fire *etc*., and the agricultural and rural development data were compiled by using the materials provided by the local forestry and agricultural committees of three major cities.

2.2 Image acquisition

This scene is near the coastal regions (Fig. 1), large-scale cloud contaminated images are quite common. Thus, we have to use some images out of the growing season, and the acquisition time frame can be extended to early October under this low latitude region (Table 1).

2.3 Image calibration and LEDAPS images processing from BJGS and USGS

Most selected Landsat time series stack (LTSS) images were downloaded from the USGS, which have been geometrically corrected to achieve sub-pixel geolocation accuracy and have high levels of radiometric consistency achieved using best available calibration coefficients and calculation of reflectance in the Landsat Ecosystem Disturbance Adaptive Processing System (LEDAPS). However, for those non-standard format scenes from BJGS, which having different geo-referencing systems, a new procedure was developed to make them have the same input files of LEDAPS processing, namely, over 90 identical ground control points (GCPS) were used to co-register those images from BJGS using the 2004 image as base image by fitting a 2nd-order polynomial for projection and coordinates transformations. During the transformations, to maintain spectral fidelity, the re-sampling method of nearest neighbors was used, and five images from BJGS (Table1) were unified to the UTM projection, the sub-pixel level of the collocation accuracies among the involved images were achieved to enable the LTSS construction, and to minimize

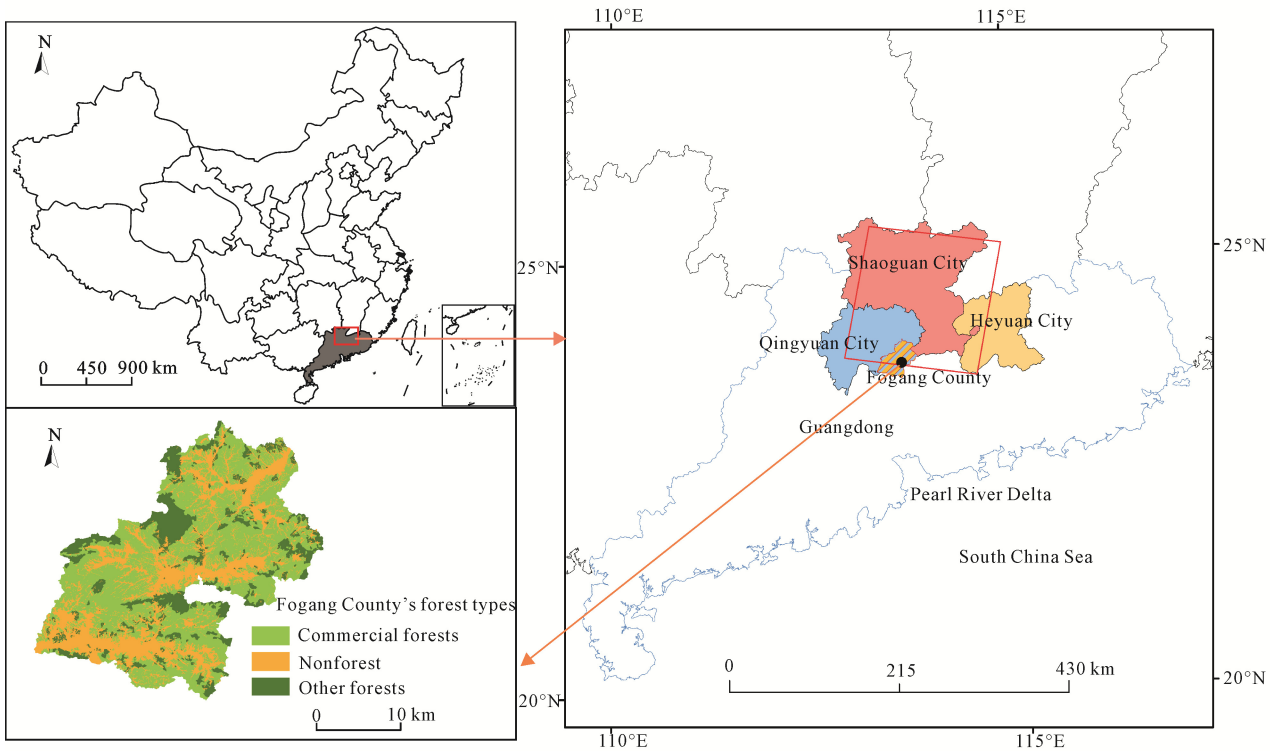

Fig. 1 Location of study site. The red line area shows our prototype study site p122r043, covering three major cities in northern Guangdong region: Shaoguan, Qingyuan, Heyuan

spurious changes arising from mis-registration errors (Townshend *et al*., 1992). Then implementing the LEDAPS to fulfill the requirement of the above- mentioned high level pre-processing algorithms and validating the efficacy of LEDAPS outputs by comparing the LEDAPS-derived spectral signatures or curves of water bodies and vegetation with those from standard spectral libraries (Shen and Li, 2014). Finally, a LTSS consisting of thirty-one Landsat images was assembled (Table 1), being utilized for mapping the disturbance and recovery products.

2.4 VCT disturbance and recovery mapping

2.4.1 Mapping and assessing disturbance and recovery over p122r043 covering northern Guangdong

The vegetation change tracker (VCT) algorithm based on an integrated forest z-score (IFZ) index which was designed by Huang *et al*. (2009) was specifically for mapping forest disturbance and recovery using LTSS or LTSS-like data sets that consist of temporally dense satellite acquisitions (Huang *et al*., 2010). Persistent forest land was defined as no major disturbance occurred during the years being monitored. Most of the errors in the persistent forest class were caused by partial disturbance events such as selective logging, understory fire, or defoliation due to insect or storm damage. The approach also did not distinguish between disturbance (mortality followed by recovery) and permanent conversion of land cover. Thus, the definition of disturbance corresponds most closely to 'gross forest cover loss' (Hansen *et al*., 2010). Considering the particularity of VCT algorithm being used to detect abrupt disturbance, and the frequent logging of the plantation in the northern Guangdong, as well the traditional silviculture and deforestation patterns in southern mountains, for example, local residents rely on forests for food, fuel and medicine, we used the VCT to monitor these forest changes and classified each pixel as forest, non-forest, water, and flagged the year of disturbance.

The disturbance year map product summarizes forest cover changes that have occurred during the observation period (1986–2015). The definitions of the disturbance map legend are summarized in Table 2. To focus on the analytical pattern of forest versus non-forest, the original seven classes in the disturbance map were aggregated. Table 2 illustrates the criteria for this aggregation. In detail, class 2 (persisting forests) and class 5 (probable

Table 1 Landsat TM/ETM+ scenes used in this analysis (p122r043)

Year/DOY (Day of year)	Satellite	Sensor	Source
1986307	Landsat 5	TM	EROS
1988313	Landsat 5	TM	BJGS
1990206	Landsat 5	TM	EROS
1992212	Landsat 5	TM	BJGS
1993278	Landsat 5	TM	EROS
1994313	Landsat 5	TM	BJGS
1995284	Landsat 5	TM	EROS
1996159	Landsat 5	TM	EROS
1997305	Landsat 5	TM	BJGS
1998228	Landsat 5	TM	BJGS
1999255, 1999287	Landsat 7	ETM+	EROS
2000258	Landsat 7	ETM+	EROS
2001252, 2001260	Landsat 5, 7	TM, ETM+	EROS
2002311	Landsat 7	ETM+	EROS
2003290	Landst 5	TM	EROS
2004277	Landsat 5	TM	EROS
2005199	Landsat 5	TM	EROS
2006266	Landsat 5	TM	EROS
2007205	Landsat 5	TM	EROS
2008208	Landsat 5	TM	EROS
2009194, 2009290	Landsat 5	TM	EROS
2010213	Landsat 5	TM	EROS
2011232	Landsat 5	TM	EROS
2012307	Landsat 7	ETM+	EROS
2013325	Landsat 7	ETM+	EROS
2014280, 2014288	Landsat 7, 8	ETM+, OLI	EROS
2015291	Landsat 8	OLI	EROS

forest with recent disturbance) were aggregated into a new forest class. Class 1 (persisting non-forest), 6 (disturbed in this year) and 7 (post-disturbance non-forest) were grouped into the non-forest class. The persisting water was kept unchanged in the aggregation. Thus, the aggregation results were used for identifying the forest changes between the observation period. From the annual forest disturbance map, we calculated the annual forest disturbance area by using the numbers of the pixels in Class 6 (Table 2), also generated the annual forest recovery area. The forest recovery area in that year was generated by intersecting forest pixels in that year with disturbance pixels before that year.

2.4.2 Mapping and assessing Fogang County's disturbance and recovery based on VCT and LandTrendr

VCT-based disturbance and recovery maps in Fogang County were clipped from the whole scene based on Fogang administration boundary. LandTrendr relies on multi-temporal segmentation to simultaneously find both abrupt events and slower, longer-term trends. And the nearly annual changing area of disturbance and recovery originating from LandTrendr has been calculated in Shen and Li (2017). The temporal span of VCT algorithm was from 1988 to 2015, while that of LandTrendr algorithm was from 1988 to 2011, because of the limitation in algorithm version. In comparison of the two changing results from both algorithms, we aimed to test their performance applying in plantation forests detection in southern China.

Table 2 Definition and aggregation of forest disturbance map derived from VCT model

Value	Class description in VCT model	Aggregated class
0	Background	Abandoned
1	Persisting non-forest	Non-forest
2	Persisting forest	Forest
4	Persisting water	Water
5	Probable forest with recent disturbance	Forest
6	Disturbed in this year	Non-forest
7	Post-disturbance non-forest	Non-forest

2.5 Accuracy assessment of VCT-developed forest disturbances

Comprehensive validation of the entire suite of VCT products has been found extremely challenging because conventional, ground or aerial photography based validation sources or reference data sets pertaining to pre- and post-disturbance and recovery processes are scarce or do not exist at the required yearly or biennial temporal frequency for the entire time period of the LTSS (Huang *et al.*, 2010; Thomas *et al*., 2011). Here, we focused on the validation of the VCT disturbance year maps. Because the spectral signals of most forest disturbances can be identified reliably by experienced image interpreters through visual examination of Landsat images acquired both before and after a particular disturbance event based on Google Earth photos (Kennedy *et al*., 2007; Huang *et al*., 2010; Thomas *et al*., 2011). For a major disturbance caused by clear cut or other stand replacing events, however, the post-disturbance pixels did not look like forests any more. After a minor disturbance, the post-disturbance pixels looked brighter and less green than the pre- disturbance pixels, but they still looked like forest pixels.

The validation aimed at major disturbance patches consisting of at least 3 × 3 continuous pixels (Landsat), because patches smaller than 3 × 3 continuous pixels were difficult for visual interpretation due to residual mis-registration errors and known impacts of sensor's point spread function (Huang *et al*., 2002). The first interpretation assessment method was through calculating a spatial agreement index (SAI) for randomly five 5 km × 5 km square plots located in the four corners of the image and centered on the image. Specifically, SAI is calculated by dividing Acd by Avc, Avc and Amd mean the areas of the visually interpreted disturbance patch and the corresponding VCT-mapped disturbance patch respectively, and Acd stands for the area of the coincidence region between Avc and Amd. The second accuracy estimation method was to create a confusion matrix (overall accuracy, kappa coefficient, and per class user's, and producer's accuracies) based on reference data sets of the above five validation sites, according to Stehman and Czaplewski, 1998. Fogang county's disturbance results were validated due to reliable ground reference data. For each of four sites, validation samples were selected using a stratified random sampling method and each class in the disturbance year map was used to define a stratum. Persisting water was included in the persisting non-forest class. We targeted 30 samples per stratum, with 27 stratums. A total of 810 validation samples were selected for each validation site. For each validation sample, all images of the target LTSS were inspected visually to determine whether it belonged to one of the 'persisting' classes or it had disturbances. The disturbance years were recorded after they were found at a sample location.

3 Results and Discussion

3.1 Validation of disturbance year map

Fig. 2 demonstrates the disturbance year map derived from the VCT algorithm and the associated five validation square plots, each with an area of 25 km^2. Table 3 list all the agreement index measures of the five plots. Measures of the spatial agreement ranged from 24.1% to 97.3%, and the majority of the measures stayed at 60% through 83% (Table 3). The validation accuracies were fully in agreement with those derived in the United States, which overall accuracy for North America Forest Disturbance (NAFD) individual time step disturbance products ranged from 77% to 86% (Thomas *et al*., 2011). There were two exceptionally low agreement value (38.1%) occurring between 2000 and 2001, (24.1%) between 2008 and 2009 in the lower right plot, respectively. When tracing back to the image from the appropriate time period we found that the VCT algorithm missed a patch of low intensity disturbances, which could be detected visually on the imagery. Also, some geometric errors originated from BJGS images undoubtedly produced some spurious changes in the disturbance year maps detected by VCT. This was likely the case for the low measure of 43.2% and 52.1% in the disturbance year of 1992 and 1994.

Table 4 provides a summary of the accuracy measures for all four validation sites in Fogang County, showing that the disturbance year maps had overall accuracy of 71.70%. The producer's and user's accuracies averaged over all classes ranged from 68.37% to 92.91% and 70.51% to 79.37%, respectively. The errors in the disturbance year products can be attributed to several factors. The first is that it is difficult to detect many non-stand clearing disturbances by the current version of the VCT; the second is the lack of ground information or high resolution data, namely, for field survey data, one reason was without effective forest survey data corresponding to annual year, only four years available sub-compartment survey data covering the Fogang County could be referred, because the national data were not opened to the public, another reason was the inaccuracy of geographic coordinates location; for reference data, only minor local clear Google Earth photos could provide high resolution examination for validation. Moreover, most of the disturbed pixels that were mapped as persisting forest by VCT were identified as non-stand clearing disturbances. Also, the disagreements were attributed to undetected thinning, crop lands and wetlands. Most of the overall accuracies and kappa values are close to those reported by Huang *et al*., (2010) and Kennedy *et al*., 2007.

3.2 Analysis of forest changes

From annual forest disturbance map generated by VCT, we generated annual forest cover, and the persisting non-forest and disturbed patches were grouped into non-forest type as annual non-forest cover (Fig. 3). Forest cover increased from 1.79×10^6 ha in 1986 to 1.99×10^6 ha in 2002, after which giving way to a decreasing trend during the period 2003 to 2010 (1.79×10^6 ha),

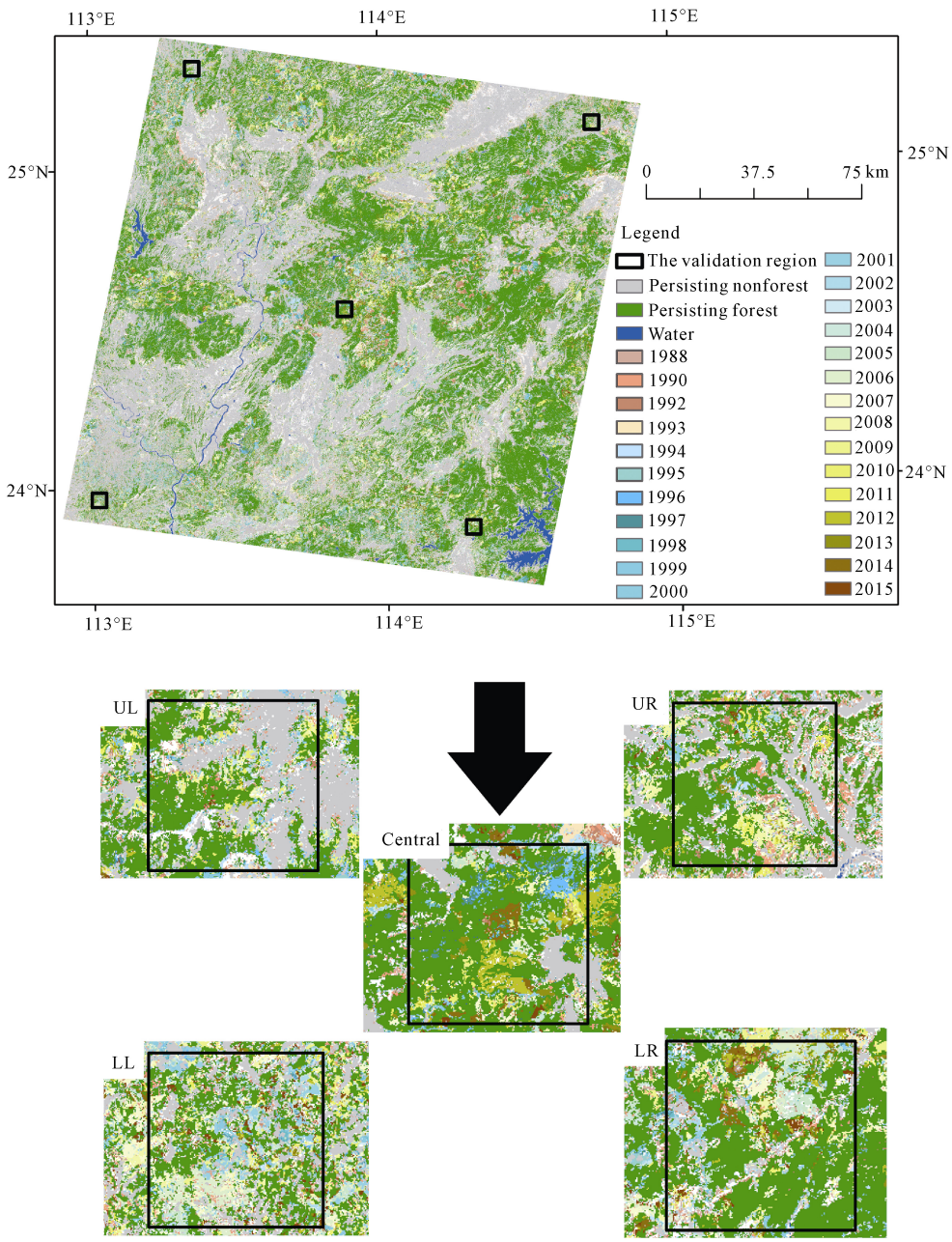

Fig. 2 The disturbance year map derived from the VCT algorithm and five validation square plots (Upper left: UL, Upper right: UR, Lower left: LL, Lower right: LR)

with that an increasing trend was reported from 1.86 × 10^6 ha in 2011 to 1.89 × 10^6 ha in 2015 (Fig. 4). Noteworthy, the trend was characterized by a subtle fluctuation before year 2002 (Fig. 4). There was a small decrease of forest area from 1.79 × 10^6 ha in 1986 to 1.72 × 10^6 ha in 1988, followed by a rising up to 1.84 × 10^6 ha in 1993, after which a slight decrease reached to 1.82 × 10^6 ha in 1994.

3.3 Forest disturbance and recovery year maps and changes in forest disturbance and recovery rate

3.3.1 Northern Guangdong region

For the acquisition year of each image in a LTSS, a disturbance rate (%) was calculated as the ratio of the pixels disturbed in that year over the total number of forest pixels (Huang *et al.*, 2009). Likewise, the recovery rate (%) was calculated by dividing the recovery pixels in

Table 3 Spatial agreement measures of the five square plots on forest disturbance year map

Upper left plot		Upper right plot		Lower left plot		Lower right plot		Central plot	
DY	AM (%)	DY	AM (%)	DY	AM (%)	DY	AM (%)	DY	AM (%)
1986		1986		1986		1986		1986	
1988	63.8	1988	75.8	1988	81.6	1988	73.7	1988	66.4
1990	92.1	1990		1990		1990	97.3	1990	
1992		1992	62.8	1992		1992		1992	43.2
1993	66.9	1993	89.2	1993		1993		1993	78.8
1994	70.9	1994	62.8	1994	52.1	1994	64.1	1994	67.3
1995		1995		1995	63.8	1995	55.1	1995	58.2
1996		1996	67.4	1996		1996		1996	65.8
1997		1997		1997		1997		1997	60.9
1998		1998		1998		1998		1998	
1999		1999	75.3	1999		1999		1999	
2000		2000	53.2	2000		2000		2000	
2001		2001		2001	73.0	2001	38.1	2001	
2002		2002		2002		2002	53.1	2002	
2003	66.0	2003		2003		2003		2003	
2004		2004		2004		2004		2004	
2005		2005		2005	74.6	2005		2005	
2006		2006		2006	55.4	2006	62.6	2006	
2007		2007	78.0	2007	63.7	2007	69.8	2007	
2008		2008	53.0	2008	59.8	2008	82.6	2008	43.8
2009		2009	64.1	2009		2009	24.1	2009	74.6
2010		2010	64.3	2010		2010		2010	
2011	66.3	2011	58.8	2011		2011	77.4	2011	77.1
2012	65.1	2012	54.3	2012		2012	63.1	2012	55.3
2013		2013		2013		2013	56.0	2013	84.1
2014		2014		2014	54.3	2014	67.1	2014	60.1
2015		2015		2015	72.0	2015	80.1	2015	73.6

Notes: DY: disturbance year; AM(%): agreement measure; The blank cells (no data) in the table were principally attributed to lack of data due to cloud cover, or no disturbance detected by VCT

Table 4 Confusion matrix for the VCT derived disturbance year map

VCT	Persistent forest	Persistent nonforest	Average disturbed forest	User's accuracy (%)
Persistent forest	92.61	0.79	3.79	79.37
Persistent nonforet	0.49	90.84	6.58	73.45
Average disturbed forest	1.08	1.17	68.37	70.51
Produce's accuracy (%)	92.61	90.84	68.37	
Overall accuracy (%)	71.50	Kappa	0.68	

that year over the total number of forest pixels. Fig. 5 displays the variation of annual forest disturbance rate and recovery rate. Because it was not possible to know the status in the pre-observation category and therefore forest disturbance and recovery rate in 1986 was excluded from Fig. 5.

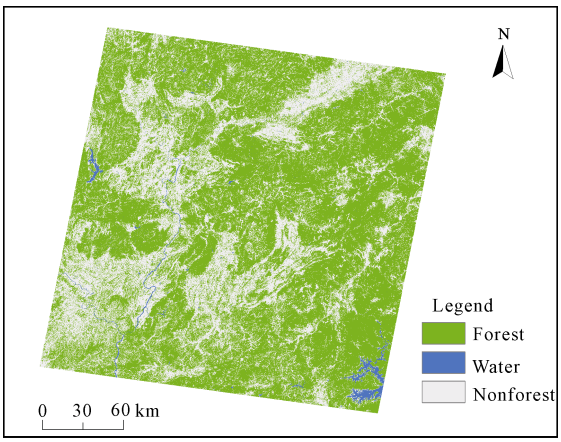

Fig. 3 Example of spatial distribution of forest changes mapped in 2015

Fig. 5 illustrates that forest disturbance rates change trend was a decline first, followed by an increase, and then giving way to a decline. An undulated and gentle decreasing trend of disturbance rates from the highest value of 3.95% to the lowest value of 0.76% occurred between 1988 and 2001, disturbance rate of 4.51% in 1994 was a notable anomaly, while after 2001 there was a sharp ascending change, except for 2006, forest disturbance rate spiked in 2007(5.84%). After that, there were a significant decreasing trend up to the lowest value of 1.96% in 2011 and a slight ascending from 2011 to 2015 (2.59%). Two obvious spikes in post-disturbance recovery rates occurred in 1995 (0.26%) and 2008 (0.41%). Overall, forest recovery rates were lower than forest disturbance rates.

We calculated the forest recovery areas between seven time intervals of almost every five years from 1988 to 2015 (Fig. 6), year intervals were 1988 to 1992, 1992 to 1996, 1996 to 2000, 2000 to 2004, 2004 to 2008, 2008 to 2012, and 2012 to 2015, respectively. Results showed that the obvious highest recovery area

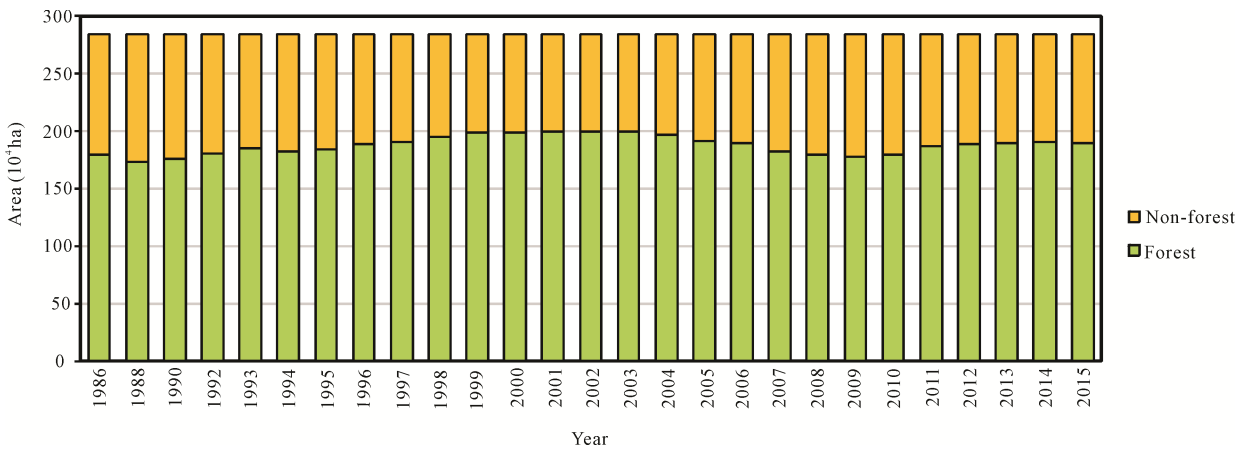

Fig. 4 Forest areas changing with time by VCT

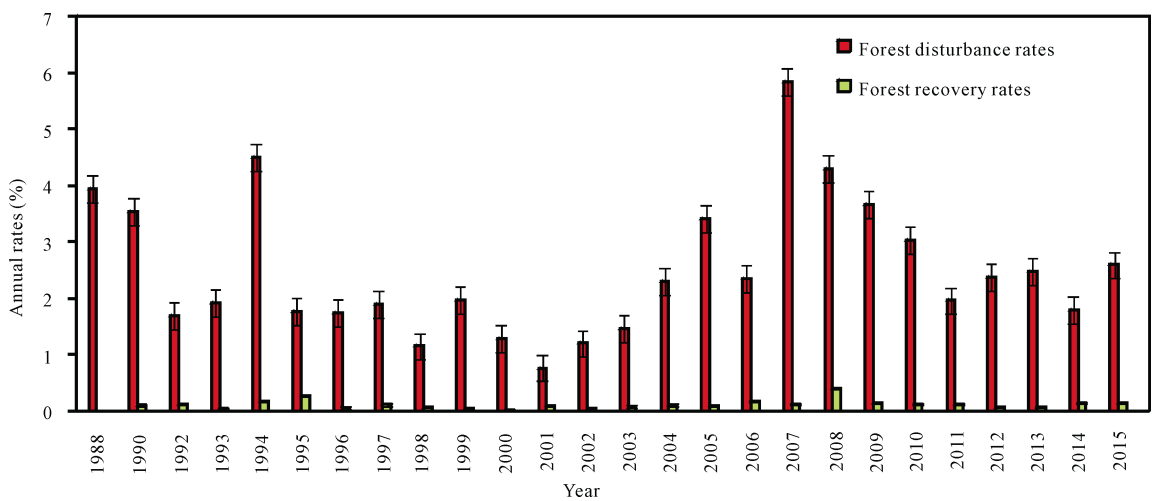

Fig. 5 Temporal variation of the annual forest disturbance and recovery rate

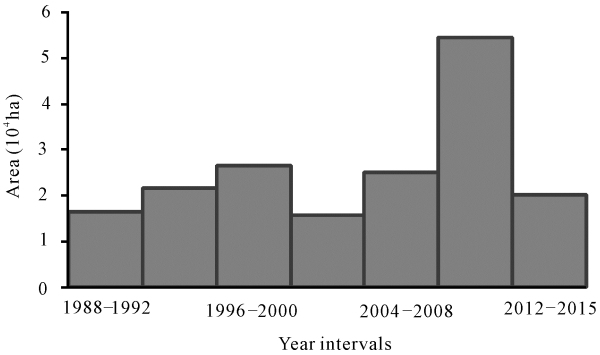

Fig. 6 Areas of forest recovery year change map within seven time intervals from 1988 to 2015

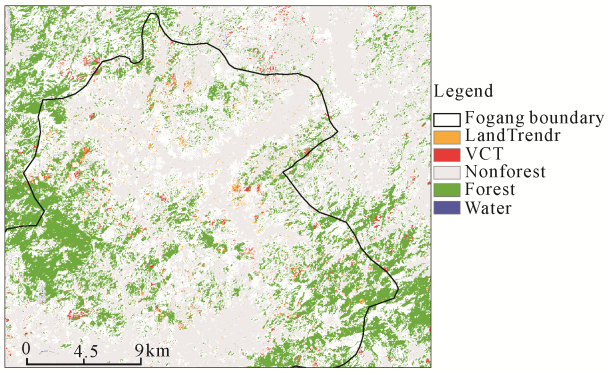

Fig. 7 Fogang County with VCT and LandTrendr forest disturbance in northern Guangdong

was 5.46 × 10^4 ha from 2008 to 2012, 2.66 × 10^6 ha from 1996 to 2000 was the second, which was higher than that of 2.50 × 10^6 ha from 2004 to 2008, the lowest value of 1.57 ×10^4 ha was witnessed between 2000 to 2004.

Missing three years of 1987, 1989 and 1991 impacted the calculation of annual recovery rates from the annual disturbance map. Similarly, Landsat images in 1988, 1994, and 1997 from BJGS were collected on November 8th, November 9th, November 1st, respectively, which were time of late autumn or the early winter in this low-latitude region. Thus, the deciduous forests during this time likely represented near leaf-off status, which led the VCT algorithm to erroneously flag these sites as areas of change. The different imagery preprocessing means between BJGS and USGS also resulted in estimation errors. The cloud cover was high in 1996, 1997, 1998 and 1999. Also underestimation of partial disturbances may introduce biases to disturbance rates calculated from those products. The overestimate of disturbance rate would come from the confusion between mixed urban and tree areas.

3.3.2 Fogang county's VCT and LandTrendr forest disturbance and recovery

Fast growing and high yield commercial forests and economic forests are dominant tree in Fogang County (Fig. 1). Both algorithms could identify an abrupt event (harvesting) (Fig. 7). VCT-based results (Fig. 8a) showed that an annual disturbance of near 1000 ha was witnessed for most years, and an annual disturbance of over 2000 ha occurred in 1988, 2003, 2004, 2005, 2006, 2007, 2008, 2009, 2010, and 2015. Particularly, the disturbance area of 2007 exceeded 6000 ha. In comparison to forest disturbance, forest recovery areas were also changing obviously. Through a trend analysis of forest disturbance and recovery in Fogang County, forest recovery area was significant less than disturbance area. LandTrendr-based results (Fig. 8b) indicated an annual disturbance area of 1000 ha for most years of the study, and an annual disturbance of over 2000 ha occurred in 2002, 2004, 2005, 2006, 2007, and 2009. Particularly, the disturbance of 2007 exceeded 6000 ha. In comparison to forest disturbance, forest recovery areas were relatively stable (Shen and Li, 2017). Overall, both algorithms reported that forest disturbance and recovery areas in the late 1980s through 1990s were less than those after 2000, and the trend was lower than that after 2000. Since 2000, the forest disturbance areas have gradually increased, with a slight increase in forest recovery, but the overall magnitudes of forest disturbance exceeded those of forest recovery.

Both algorithms infer change on ground from changes in the spectral signal captured over time by multiple Landsat images, they do so in different ways and produced noticeably different spatial (Fig.7) and temporal (Fig. 8) patterns, with LandTrendr finding much more disturbance than VCT mostly like the results in Schroeder *et al.*, 2012. Because some disturbance from non-forested areas based on LandTrendr algorithm were added in forest disturbance map. Despite these differences, both maps resulted in similar accuracy metrics when compared with the satellite interpretations of disturbance (VCT overall accuracy 78%; LandTrendr overall accuracy 77%).

3.4 Driving forces analysis of forest changes

The 'Green Guangdong' afforestation plan was estab-

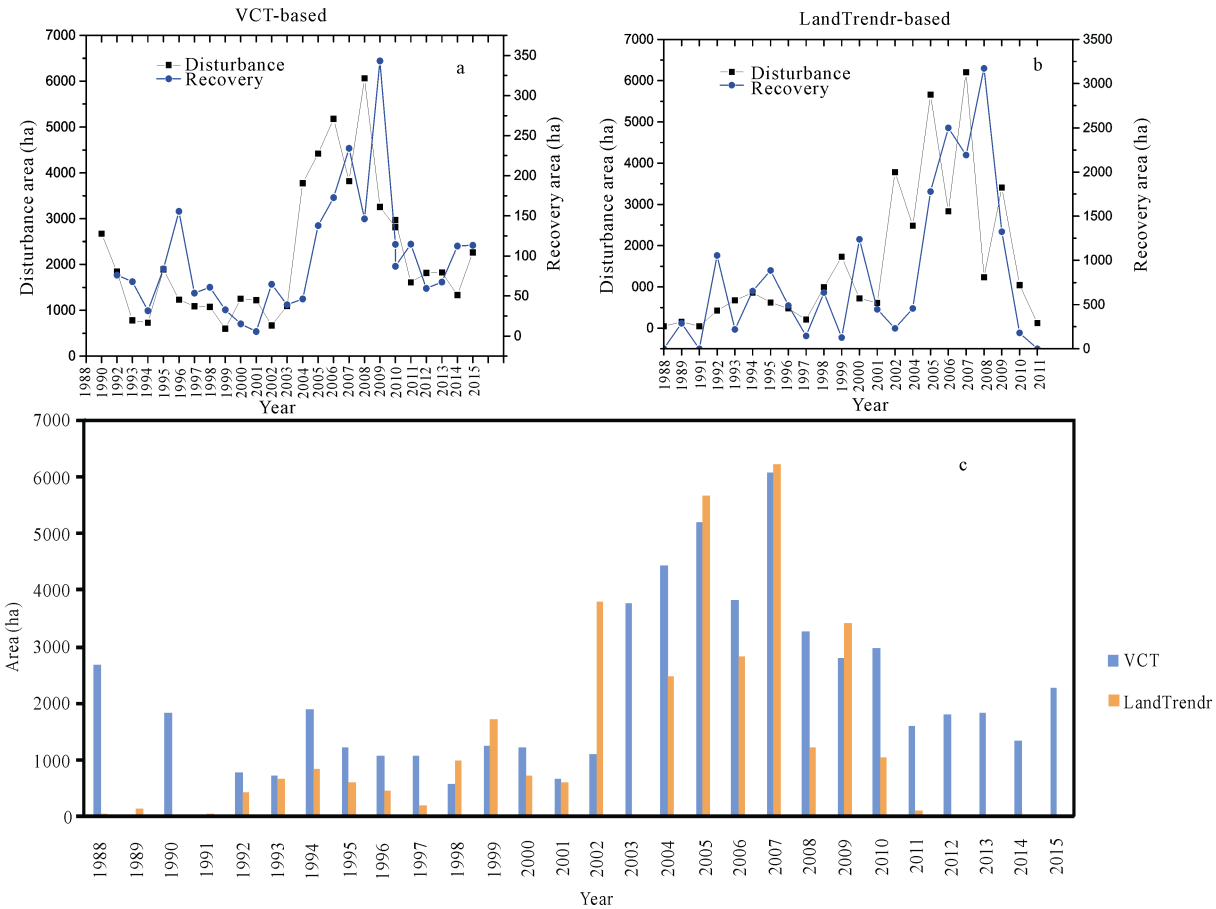

Fig. 8 Forest disturbance and recovery area changing in Fogang County. a) VCT; b) LandTrendr; c) Area of disturbance (ha) mapped by VCT and LandTrendr

lished in the 1980s and resulted in mountain forests regrowth in the early 1990s, especially in 1992. At the beginning of mid-1990s, due to the blind of short-term economic benefit, an amount of eucalyptus species were introduced to the northern Guangdong. As the fast-growing and high-yield plantations have short rotation cycle and need to be cut for a new regeneration (Shen *et al*., 2016). Results showed that forest area constantly rose in the 1980s, and within the fast-growing fertility forests planted in the 1990s, the seedling grew to the mature forest, made the forest area cover of year 2002 reach the peak (Fig. 4). Forest disturbance rate in 1994 was higher as a result of the traditional cultivation of clear cutting then prescribed burning for land preparation responding to the implementation of eucalyptus construction plan (Fig. 5). Harvesting led the disturbance rates obviously rising since 2006. The reason was that the fast-growing productive trees being logged at a six years rotation period and the new reforestation came into the next cutting period. Furthermore, after 2000, the permission for a low slope development plan and mountainous urbanization increase could explain the gradually decreasing forest area and the increasing forest disturbance rate. Meanwhile, to protect water source forests and conservation forests, the eucalyptus plan was banned by local government, but some plantations were remaining. Furthermore, afforestation on the barren mountains, cutting-blank, fire-slash, inefficient forest lands was conducted, which together led to a slight rising of recovery rates after 2000 (Shen *et al*., 2016). The rain and ice snow storm in mid-January to early February 2008 destroyed 30 years of hard work from the 1980s to reforest the region (Zhou *et al*., 2011), accounting for one-tenth of China's forests and plantations, which was roughly equivalent to the number of hectares that were reforested between 2003 and 2006, according to China's State Forestry Administration (Stone, 2008). The statistical materials from the local government and South China Botanical Garden in Guangzhou showing that restoration plans after snow

disaster helped the forest recover fast (Stone, 2008).

3.5 Some difficulties and uncertainty

Forest types here are dominated by evergreen forests, to some extent, alleviating the effects of phenology. Images acquired during or near the leaf-off season were considered, because the area in northern Guangdong where trees grow rapidly, even a stand clearing harvest can be replaced by thick young forests on just a few years, which are often spectrally similar to undisturbed forests. As a result, a harvest event may not be spectrally detectable if no images are acquired immediately after the event, while nearly annual record rather than biennial time series stacks being used had proved the results would have been incrementally improved (Thomas *et al.*, 2011). Additionally, the current version of VCT cannot map the disturbance types or sources individually, some additional analyses are needed to separate disturbance sources to enable further understanding of catalysts for disturbance (Kennedy *et al.*, 2010; Kennedy *et al.*, 2012; Zhu *et al.*, 2012; Vogelmann *et al.*, 2012; Neigh *et al.*, 2014; Zhao *et al.*, 2015). Some uncertainties between forest disturbance and recovery, forest ecosystem (biomass, carbon stock) (Frolking *et al.*, 2009), urbanization and climate (Dale *et al.*, 2001; Pei *et al.*, 2015) still existed and need to be solved further.

4 Conclusions

This work has developed a forest disturbance and recovery history using a vegetation change tracker (VCT) model within the plantation in northern Guangdong based on an assembled LTSS consisting of annual Landsat time series observations spanning from 1986 to 2015. It has demonstrated that VCT has a stable mapping abrupt disturbance although implementing VCT confronts more difficulties outside of the USA. And VCT and LandTrendr algorithms utilized in Fogang County have been conducted, with LandTrendr finding mostly much more disturbance than VCT. The mapped forest change patterns in northern Guangdong province are not only highly related to Chinese economic, demographic, environmental and political policies, but also to some extreme catastrophic events under the special geographical conditions. It is our belief that popularizing the automated algorithms is beneficial to create a clear sight of forest disturbance and recovery histories and provide a critical component for assessing forest management, forest carbon sequestration and planning biodiversity conservation under climate change.

Acknowledgements

Special thanks need to go to the USGS EROS Center and the remote sensing ground station of Beijing, both provided the Landsat images. The authors also thank the Guangdong Provincial Center for Forest Resources Monitoring and Fogang forestry staff, thank Dr. Chengquan Huang, Dr. Min Feng in University of Maryland and Dr. Zhiqiang Yang in Oregon State University in provision of the aid of algorithms.

References

Chen Xingliang, Ju Qian, Lin Kunlun, 2014. Development status' issues and countermeasures of China's Plantation. *World Forestry Research*, 27(6): 54–59. (in Chinese)

Cohen W B, Yang Z Q, Stehman S V *et al.*, 2016. Forest disturbance across the conterminous United States from 1985–2012: the emerging dominance of forest decline. *Forest Ecology and Management*, 360: 242–252. doi: 10.10 16/j.foreco.2015.10.042

Coppin P R, Jonckheere I, Nackaerts K *et al*., 2004. Digital change detection methods in ecosystem monitoring: a review. *Journal of Remote Sensing*, 25(9): 1565–1596. doi: 10.1080/0143116031000101675

DaleV H, Joyce L A, McNulty S *et al*., 2001. Climate change and forest disturbances: climate change can affect forests by altering the frequency, intensity, duration, and timing of fire, drought, introduced species, insect and pathogen outbreaks, hurricanes, windstorms, ice storms, or landslides. *BioScience*, 51(9): 723–734. doi: 10.1641/0006-3568 (2001)051[0723:CCAFD]2.0.

Edwards D P, Tobias J A, Sheil D *et al.*, 2014. Maintaining ecosystem function and services in logged tropical forests. *Trends in Ecology & Evolution*, 29(9): 511–520. doi: 10.1016/j.tree.2014.07.003

Fang Jingyun, Chen Anping, 2001. Dynamic forest biomass carbon pools in China and their significance. *Acta Botanica Sinica*, 43(9): 967–973. (in Chinese)

Frolking S, Palace M W, Clark D B *et al.*, 2009. Forest disturbance and recovery: a general review in the context of spaceborne remote sensing of impacts on aboveground biomass and canopy structure. *Journal of Geophysical Research*, 114, G00E02. doi: 10.1029/2008JG000911

Goward S N, Masek J G, Cohen W *et al*., 2008. Forest disturbance and North American carbon flux. *EOS Transactions*, *American Geophysical Union*, 89: 105−106.

Huang Congde, Zhang Guoqing, 2009. Impact factors of carbon

sequestration in artificial forest carbon stock. *World Forestry Research*, 22(2): 34–38.

Huang C Q, Townshend J R G, Liang S L *et al*., 2002. Impact of sensor's point spread function on land cover characterization: assessment and deconvolution. *Remote Sensing of Environment*, 80: 203–212. doi: 10.1016/S0034 -4257(01)00298-X

Huang C Q, Goward S N, Schleeweis K *et al*., 2009. Dynamics of national forests assessed using the Landsat record: case studies in eastern United States. *Remote Sensing of Environment*, 113: 1430−1442. doi: 10.1016/j.rse.2008.06.016

Huang C Q, Goward S N, Masek J G *et al*., 2010. An automated approach for reconstructing recent forest disturbance history using dense Landsat time series stacks. *Remote Sensing Environment*, 114: 183−198. doi: 10.1016/j.rse. 2009. 08.017

Kennedy R E, Cohen W B, Schroeder T A, 2007. Trajectory-based change detection for automated characterization of forest disturbance dynamics. *Remote Sensing Environment*, 110: 370–386. doi: 10.1016/j.rse.2007.03.010

Kennedy R E, Yang Z Q, Cohen W B, 2010. Detecting trends in forest disturbance and recovery using yearly Landsat time series: 1, LandTrendr-Temporal segmentation algorithms. *Remote Sensing Environment*, 114: 2897−2910. doi: 10.1016/j.rse.2010.07.008

Kennedy R E, Yang Z Q, Cohen W B *et al*., 2012. Spatial and temporal patterns of forest disturbance and growth within the area of the Northwest Forest Plan. *Remote Sensing Environment*, 122: 117−133. doi: 10.1016/j.rse.2011.09.024

Kennedy R E, Yang Z Q, Braaten J *et al*., 2015. Attribution of disturbance change agent from Landsat time-series in support of habitat monitoring in the Puget Sound region, USA. *Remote Sensing of Environment*, 166: 271–285. doi: 10.1016/j.rse.2015.05.005

Levers C, Verkerk P J, Müller D *et al*., 2014. Drivers of forest harvesting intensity patterns in Europe. *Forest Ecology and Management*, 315: 160–172. doi: 10.1016/j.foreco.2013.12.030

Li M S, Huang C Q, Zhu Z L *et al*., 2009a. Assessing rates of forest change and fragmentation in Alabama, USA, using the vegetation change tracker model. *Forest Ecology and Management*, 257: 1480−1488. doi: 10.1016/j.foreco.2008. 12.023

Li M S, Huang C Q, Zhu Z L *et al*., 2009b. Use of remote sensing coupled with a vegetation change tracker model to assess rates of forest change and fragmentation in Mississippi, USA. *International Journal of Remote Sensing*, 30: 6559–6574. doi: 10.1080/01431160903241999

Lu D S, Mausel P, Brondízio E *et al*., 2004. Change detection techniques. *International Journal of Remote Sensing*, 25(12): 2365–2401. doi: 10.1080/0143116031000139863

Ma Z Q, Hartmann H, Wang H M *et al*., 2013. Carbon dynamics and stability between native Masson pine and exotic slash pine plantations in subtropical China. *European Journal of Forest Research*, 133(2): 307–321. doi: 10.1007/s10342- 013-0763-5

Mas J F, 1999. Monitoring land-cover changes: a comparison of change detection techniques. *International Journal of Remote Sensing*, 20(1): 139–152. doi: 10.1080/014311699213659

Masek J G, Goward S N, Kennedy R E *et al*., 2013. United States forest disturbance trends observed with Landsat time series. *Ecosystems*, 16: 1087–1104. doi: 10.1007/s10021-013-9669-9

Neigh C S R, Bolton D K, Williams J J *et al*., 2014. Evaluating an automated approach for monitoring forest disturbances in the Pacific Northwest from logging, fire and insect outbreaks with Landsat time series data. *Forests*, 5: 3169–3198. doi: 10.3390/f5123169

Pei F S, Li X, Liu X P *et al*., 2015. Exploring the response of net primary productivity variations to urban expansion and climate change: A scenario analysis for Guangdong Province in China. *Journal of Environmental Management*, 150: 92–102. doi: 10.1016/j.jenvman.2014.11.002

Pflugmacher D, Cohen W B, Kennedy R E, 2012. Comparison between Landsat derived disturbance history (1972–2010) to predict current forest structure. *Remote Sensing of Environment*, 122: 146–165. doi: 10.1016/j.rse.2011.09.025

Piao S L, Fang J Y, Ciais P *et al*., 2009. The carbon balance of terrestrial ecosystem in China. *Nature*, 458: 1009–1013. doi: 10.1038/nature07944

Roy D P, Wulder M A, Loveland T R *et al.*, 2014. Landsat-8: science and product vision for terrestrial global change research. *Remote Sensing of Environment*, 145: 154 –172. doi: 10.1016/j.rse.2014.02.001

Schroeder T A, Moisen G G, Healey S P *et al*., 2012. Adding value to the FIA inventory: combining FIA data and satellite observations to estimate forest disturbance. In: Morin, Randall S, Liknes, Greg C, comps. Moving from status to trends: Forest Inventory and Analysis (FIA) symposium 2012; [CD-ROM]: 143–148.

Schroeder T A, Healey S P, Moisen G G *et al*., 2014. Improving estimates of forest disturbance by combining observations from Landsat time series with US Forest Service Forest Inventory and Analysis data. *Remote Sensing of Environment*, 154: 61–73. doi:10.1016/j.rse.2014.08.005

Shen Wenjuan, Li Mingshi, 2014. Method for Landsat dense time series data format unification and surface reflectance conversion. *Remote Sensing for Land & Resources*, 26(4): 78–84. doi: 10.6046/gtzyyg.2014.04.13 (in Chinese)

Shen W J, Li M S, Huang C Q *et al*., 2016. Quantifying live aboveground biomass and forest disturbance of mountainous natural and plantation forests in northern Guangdong, China, based on multi-temporal Landsat, PALSAR and field plot data. *Remote sensing*, 8(7): 595. doi: 10.3390/rs8070595

Shen Wenjuan, Li Mingshi, 2016. Mapping disturbance and recovery of plantation forests in southern China using yearly Landsat time series observations. *Acta Ecologica Sinica*, 37(5): 1438-1449. doi: 10.5846/stxb201510142074 (in Chinese)

Stehman S V, Czaplewski R L, 1998. Design and analysis for thematic map accuracy assessment: Fundamental principles. *Remote Sensing of Environment*, 64: 331–344. doi: 10.1016/S0034-4257(98)00010-8

Stone R, 2008. Ecologists report huge storm losses in China's forests. *Science*, 319: 1318–1319. doi: 10.1126/science. 319. 5868.1318

Thomas N E, Huang C Q, Goward S N *et al*., 2011. Validation of North American forest disturbance dynamics derived from Landsat time series stacks. *Remote Sensing of Environment*, 115: 19–32. doi:10.1016/j.rse.2010.07.009

Townshend J R G, Justice C O, McManus J, 1992. The impact of misregistration on change detection. *IEEE Transactions on Geoscience and Remote Sensing*, 30(5): 1054–1060. doi: 10.1109/36.175340

Turner D P, Ritts W D, Kennedy R E *et al*., 2015. Effects of harvest, fire, and pest/pathogen disturbances on the West Cascades ecoregion carbon balance. *Carbon Balance and Management*, 10: 12. doi: 10.1186/s13021-015-0022-9

Vogelmann J E, Xian G, Homer C *et al*., 2012. Monitoring gradual ecosystem change using Landsat time series analyses: case studies in selected forest and rangeland ecosystems. *Remote Sensing of Environment*, 122: 92−105. doi: 10.1016/j.rse.2011.06.027

Woodcock C E, Allen R, Anderson M *et al*., 2008. Free access to Landsat imagery. *Science*, 320(5879): 1011. doi: 10. 1126/science.320.5879.1011a.

Wu Zhijun, Su Dongkai, Niu Lijun *et al*., 2016. Effects of logging intensity on structure and composition of a broadleaf-korean pine mixed forest on Changbai Mountains, Northeast China. *Chinese Geographical Science*, 26(1): 59−67. doi: 10.1007/s11769-015-0

Zhao F, Huang C Q, Zhu Z L, 2015. Use of vegetation change tracker and support vector machine to map disturbance types in greater yellowstone ecosystem in a 1984−2010 Landsat time series. *IEEE Geoscience and Remote Sensing Letters*: 1–5. doi: 10.1109/LGRS.2015.2418159

Zhou B Z, Gu L H, Ding Y H *et al*., 2011. The great 2008 Chinese ice storm: its socioeconomic - ecological impact and sustainability lessons learned. *Bulletin of the American Meteorological Society*, 92(1): 47–60. doi: 10.1175/2010 BAMS2857.1

Zhu Z, Woodcock C E, Olofsson P, 2012. Continuous monitoring of forest disturbance using all available Landsat imagery. *Remote Sensing of Environment*, 122: 75–91. doi: 10.1016/j.rse.2011.10.030